

U-Load Dextramer®

Build multimers with your choice of peptide and peptide-receptive MHC I and MHC II alleles.



TLR-Induced IL-12 and CCL2 Production by Myeloid Cells Is Dependent on Adenosine A₃ Receptor –Mediated Signaling

This information is current as of February 26, 2022.

Céline van der Putten, Jennifer Veth, Lejla Sukurova, Ella A. Zuiderwijk-Sick, Elles Simonetti, Hans J. P. M. Koenen, Saskia M. Burm, Johannes M. van Noort, Ad P. IJzerman, Sacha A. F. T. van Hijum, Dimitri Diavatopoulos and Jeffrey J. Bajramovic

J Immunol 2019; 202:2421-2430; Prepublished online 25 February 2019;
doi: 10.4049/jimmunol.1800618
<http://www.jimmunol.org/content/202/8/2421>

Supplementary Material <http://www.jimmunol.org/content/suppl/2019/02/22/jimmunol.1800618.DCSupplemental>

References This article **cites 43 articles**, 15 of which you can access for free at:
<http://www.jimmunol.org/content/202/8/2421.full#ref-list-1>

Why *The JI*? Submit online.

- **Rapid Reviews! 30 days*** from submission to initial decision
- **No Triage!** Every submission reviewed by practicing scientists
- **Fast Publication!** 4 weeks from acceptance to publication

**average*

Subscription Information about subscribing to *The Journal of Immunology* is online at:
<http://jimmunol.org/subscription>

Permissions Submit copyright permission requests at:
<http://www.aai.org/About/Publications/JI/copyright.html>

Email Alerts Receive free email-alerts when new articles cite this article. Sign up at:
<http://jimmunol.org/alerts>



TLR-Induced IL-12 and CCL2 Production by Myeloid Cells Is Dependent on Adenosine A₃ Receptor–Mediated Signaling

Céline van der Putten,* Jennifer Veth,* Lejla Sukurova,* Ella A. Zuiderwijk-Sick,* Elles Simonetti,[†] Hans J. P. M. Koenen,[†] Saskia M. Burm,* Johannes M. van Noort,[‡] Ad P. IJzerman,[§] Sacha A. F. T. van Hijum,^{¶,||} Dimitri Diavatopoulos,[†] and Jeffrey J. Bajramovic*

TLR-induced signaling potently activates cells of the innate immune system and is subject to regulation at different levels. Inflammatory conditions are associated with increased levels of extracellular adenosine, which can modulate TLR-induced production of cytokines through adenosine receptor–mediated signaling. There are four adenosine receptor subtypes that induce different signaling cascades. In this study, we demonstrate a pivotal contribution of adenosine A₃ receptor (A₃R)–mediated signaling to the TLR4-induced expression of IL-12 in different types of human myeloid APC. In dendritic cells, IL-12 and CCL2 responses as evoked by TLR2, 3, 4, 5, and 8, as well as IL-12 responses evoked by whole pathogens, were all reduced when A₃R-mediated signaling was blocked. As a result, concomitant production of IFN- γ and IL-17 by T cells was significantly inhibited. We further show that selective inhibition of A₃R-mediated signaling reduced TLR-induced phosphorylation of the transcription factor STAT1 at tyrosine 701. Next-generation sequencing revealed that A₃R-mediated signaling controls the expression of metallothioneins, known inhibitors of STAT1 phosphorylation. Together our results reveal a novel regulatory layer of innate immune responses, with a central role for metallothioneins and autocrine/paracrine signaling via A₃Rs. *The Journal of Immunology*, 2019, 202: 2421–2430.

Toll-like receptors are evolutionary conserved pattern recognition receptors expressed by different cell lineages of the immune system (1). In myeloid cells, agonist recognition by TLRs initiates a cascade of intracellular signaling events that ultimately culminate in the activation of transcription factors such as NF- κ B and AP-1 (2–4). These transcription factors induce the expression of inflammatory soluble mediators like TNF- α , IL-12, and CCL2, as well as of molecules involved in Ag presentation (1, 5).

The purine nucleoside adenosine is a known regulator of inflammatory responses (6, 7). During inflammatory conditions, intracellular and extracellular adenosine levels rapidly rise. Extracellular adenosine interacts with four G protein–coupled

adenosine receptor (ADORA) subtypes. Adenosine A₁ and A₃ receptors (A₁R and A₃R) are coupled to Gi proteins and mediate opposite effects to adenosine A_{2A} and A_{2B} receptors (A_{2A}R and A_{2B}R) that are coupled to Gs proteins. The ADORA expression pattern, which is highly dynamic, therefore orchestrates the cellular response to adenosine (8, 9).

ADORA-mediated signaling also modulates innate immune responses induced by myeloid cells. A_{2A}R-mediated signaling inhibits TLR-induced NF- κ B activation and concomitant production of cytokines in macrophages and microglia (10–13). Recently, our group described that A₃R-mediated signaling counteracts A_{2A}R-mediated inhibitory signaling (14). Data from the same study suggested that A₃R-mediated signaling was also directly involved in TLR-induced cytokine responses.

In this study, we show that A₃R-mediated signaling contributes to IL-12 and CCL2 production as induced by a broad range of TLRs and pathogens and has downstream effects on T cell responses to whole pathogens. Dendritic cell (DC)–CD4⁺ T cell coinoculation experiments demonstrate that bacterial and fungal-induced IFN- γ and IL-17 responses are significantly inhibited when they were evoked in the presence of an A₃R antagonist. Next-generation sequencing of mRNA expression profiles revealed that A₃R-mediated signaling controls the expression levels of metallothioneins, which in turn can inhibit the phosphorylation of the transcription factor STAT1. These results demonstrate that endogenously produced adenosine provokes A₃R-dependent signaling, which essentially contributes to the TLR-induced cytokine response profile.

Materials and Methods

Reagents

Adenosine A₁R antagonist 8-cyclopentyl-1,3-dipropylxanthine (DPCPX), adenosine A_{2A}R antagonist 7-(2-phenylethyl)-5-amino-2-(2-furyl)-pyrazolo-[4,3-e]-1,2,4-triazolo[1,5-c]pyrimidine (SCH58261), adenosine A_{2B}R antagonist

*Alternatives Unit, Biomedical Primate Research Centre, 2288 GJ Rijswijk, the Netherlands; [†]Laboratory of Pediatric Infectious Diseases, Radboud Centre for Infectious Diseases, Radboud University Medical Centre, 6525 GA Nijmegen, the Netherlands; [‡]Delta Crystallon, 2333 CK Leiden, the Netherlands; [§]Division of Medicinal Chemistry, Leiden Academic Centre for Drug Research, 2333 CC Leiden, the Netherlands; [¶]Bacterial (Meta)genomics, Centre for Molecular and Biomolecular Informatics, Radboud University Medical Centre, 6525 GA Nijmegen, the Netherlands; and ^{||}NIZO, 6718 ZB Ede, the Netherlands

ORCID: 0000-0003-0836-8590 (L.S.); 0000-0002-1182-2259 (A.P.I.); 0000-0002-6504-3437 (J.J.B.).

Received for publication May 1, 2018. Accepted for publication January 16, 2019.

The sequences presented in this article have been submitted to the Gene Expression Omnibus under accession number GSE125747.

Address correspondence and reprint requests to Dr. Jeffrey J. Bajramovic, Alternatives Unit, Biomedical Primate Research Centre, Lange Kleiweg 161, 2288 GJ Rijswijk, the Netherlands. E-mail address: bajramovic@bprc.nl

The online version of this article contains supplemental material.

Abbreviations used in this article: A_{2A}R, adenosine A_{2A} receptor; A_{2B}R, adenosine A_{2B} receptor; ADORA, adenosine receptor; A₁R, adenosine A₁ receptor; A₃R, adenosine A₃ receptor; DC, dendritic cell; ntc, nontargeting control; SAPK, stress-activated protein kinase; shRNA, short hairpin RNA; THP-1^{Δ3}, THP-1 cell transduced with A₃R-targeting shRNA; THP-1^{mtc}, THP-1 cell transduced with ntc shRNA.

Copyright © 2019 by The American Association of Immunologists, Inc. 0022-1767/19/\$37.50

8-(4-[[[4-cyanophenyl]carbamoylmethyl]oxy]phenyl)-1,3-di(*n*-propyl) xanthine hydrate (MRS1754), adenosine A₃R antagonists 9-chloro-2-(2-furanyl)-5-([phenylacetyl]amino)-[1,2,4]triazolo[1,5-*c*]quinazoline (MRS1220), and 3-ethyl-5-benzyl-2-methyl-4-phenylethynyl-6-phenyl-1,4-(±)-dihydropyridine-3,5-dicarboxylate (MRS1191; all Sigma-Aldrich, Saint Louis, MO) were diluted in DMSO, aliquoted, and stored at -20°C. The 4-methoxy-*N*-(3-[2-pyridinyl]-1-isoquinolinyl)benzamide (VUF8504) was synthesized in-house. DMSO controls were included in all functional assays.

TLR agonists used were Pam₃CSK₄ (TLR2), poly(I:C) (TLR3), LPS (TLR4), flagellin (TLR5), and CL075 (TLR8; all Invivogen, San Diego, CA). Heat-killed *Candida albicans* and heat-killed *Staphylococcus aureus* were obtained from Invivogen; *Haemophilus influenzae* strain 86-028NP [nontypeable (15)] was cultured in brain heart infusion medium at 37°C, washed, and heat-killed for 30 min at 56°C. Recombinant human IFN-γ was from Peprotech (London, U.K.), and PMA was from Sigma-Aldrich.

Cell culture

Human PBMCs were isolated from human buffy coats obtained from anonymized healthy donors (Sanquin, the Netherlands) using lymphocyte separation medium gradient centrifugation (Lymphoprep; Axis-Shield, Norway). Monocytes were isolated with anti-CD14, and T cells with anti-CD4 mAb-coated Microbeads using MACS single-use separation columns from Miltenyi Biotec (Bergisch Gladbach, Germany) as described by the manufacturer. CD4⁺ T cells were resuspended in 10% DMSO (v/v) with heat-inactivated FCS and frozen in liquid nitrogen until further use.

Purified CD14⁺ cells were resuspended in RPMI 1640 (Life Technologies, Thermo Fisher Scientific, Waltham, MA) containing 10% (v/v) FCS (Life Technologies) and penicillin 100 U/ml and streptomycin 0.1 mg/ml (Life Technologies) supplemented with ≥4 U recombinant human M-CSF/ml or ≥40 U recombinant human GM-CSF and 200 ng of recombinant human IL-4/ml (all Peprotech) to yield macrophages or DC, respectively. Half of the medium was replaced by fresh medium containing new growth factors every 3–4 d. After 6–7 d in culture, cells were used for functional assays. For the Ag presentation assays, donor-matched CD4⁺ T cells were thawed and added to DC in a ratio of 5:1 together with either VUF8504 or vehicle control. Heat-killed *Candida albicans*, heat-killed *Staphylococcus aureus*, or heat-killed *Haemophilus influenzae* strain 86-028NP (1.25 × 10⁶ CFU/well) or an equivalent volume of medium was added subsequently. Following stimulation, supernatant was isolated 24 h and 5 d later and stored at -20°C until further analysis.

THP-1 cells were cultured in RPMI 1640 supplemented with 10% (v/v) FCS, 2 mM GlutaMAX, 1 mM nonessential amino acids, 1 mM sodium pyruvate, 100 U penicillin/ml, and 0.1 mg streptavidin/ml (all Life Technologies).

Lentiviral short hairpin RNA transduction of THP-1 cells

THP-1 cells were seeded in a 96-well plate at a concentration of 1 × 10⁴ cells per well and incubated for 24 h before lentiviral short hairpin RNA (shRNA) transduction particles (SHCLNV MISSION pLKO.1-puro non-mammalian shRNA; Sigma-Aldrich) were added to the cells at different multiplicities of infection in the presence of 80 µg polybrene/ml for overnight incubation. Medium containing lentiviral particles was replaced by fresh cell culture medium and incubated for 48 h. At day 3, fresh medium containing 5 µg puromycin/ml (Invivogen) was added, and medium was refreshed 1:1 v/v every 3–4 d. After outgrowth, clones were selected and characterized.

Next-generation sequencing

The Ultra Directional RNA Library Prep Kit for Illumina (New England Biolabs, Ipswich, MA) was used to prepare and process the samples. Briefly, mRNA was isolated from total RNA using oligo(dT) magnetic beads. After fragmentation of the mRNA, cDNA synthesis was performed followed by ligation of sequencing adapters and PCR amplification. The quality and yield after sample preparation was measured with a fragment analyzer (Advanced Analytical, Heidelberg, Germany). The size of the resulting products was consistent with the expected size distribution (a broad peak between 300 and 500 bp, data not shown). Clustering and DNA sequencing using the Illumina NextSeq 500 was performed according to the manufacturer's protocols. A total of 1.6 pM of DNA was loaded and analyzed using NextSeq control software 2.0.2. Image analysis, base calling, and quality verification were performed with Illumina data analysis pipeline RTA v2.4.11 and Bcl2fastq v2.17. The reads were mapped to reference sequence Homo_sapiens.GRCh37.75 using a short-read aligner based on Burrows-Wheeler transform (mismatch rate of maximum 2%). For the 16 samples, the number of reads obtained was

between 22,537,666 and 32,979,730. The % reads of reads aligned to the reference was between 95.4 and 95.7%. Reads that aligned to multiple locations were between 7.5 and 9.4%. Reads that aligned to genes were between 60.0 and 87.8%. SAMtools 0.1.18 was used to sort and index the BAM files. The number of times a read aligned to a gene and normalized read counts in fragments per kb million were determined using in-house-developed scripts. The R package DESeq 1.10.1 was used to calculate false discovery rate-corrected *p* values for the genes differentially expressed in the tested samples.

Quantitative RT-PCR

Total cellular RNA was isolated using TriReagent (Sigma-Aldrich) according to the manufacturer's protocol. Subsequently, mRNA was reverse transcribed into cDNA using the Fermentas kit according to the manufacturer's protocol (Qiagen Benelux, Venlo, the Netherlands) using 1 µg of mRNA as template and 0.25 µg of oligo(dT)15 primers supplied with the kit. RT-PCRs were performed on the CFX96 Thermal Cycler (Bio-Rad, Hercules, CA) using primer (Life Technologies, Thermo Fisher Scientific) and probe (human Exiqon ProbeLibrary, Roche, Woerden, the Netherlands) combinations listed in Table I. Gene of interest mRNA expression levels were standardized to GAPDH expression levels using the Pfaffl method (16).

Cytokine analysis and Luminex

IL-12p40 and TNF-α levels were determined by ELISA according to the manufacturer's protocol (U-Cytech, Utrecht, the Netherlands). IL-17 and IFN-γ levels were determined by ELISA kits (IL-17; R&D Systems, IFN-γ; Sanquin, the Netherlands) according to the manufacturer's protocol. Multiplex assays were performed using a customized Non-Human Primate MILLIPLEX MAP kit (Millipore, Billerica, MA). CCL2, IL-12, IL-6, IL-8, MIP1α, MIP1β, and TNF-α levels were determined according to the manufacturer's protocol and analyzed on the Luminex 200 System (Bio-Rad).

PathScan ELISA

NF-κBp65, p-NF-κBp65 (Ser536), p-stress-activated protein kinase (SAPK)/JNK (Thr183/Tyr185), p-p38 (Thr180/Tyr182), and p-ERK1/2 (Thr202/Tyr204) levels were measured in cell lysates using PathScan ELISA Kit (Cell Signaling Technology, Beverly, MA). Cell lysates were generated according to protocol in lysis buffer provided with the kit, supplemented with protease inhibitors (Roche). Samples were stored at -80°C before use and diluted 1:1 in dilution buffer provided with the kit before incubation for 16 h at 4°C. All following steps were performed according to the manufacturer's protocol. Nonphosphorylated NF-κBp65 levels were used as reference values for each sample.

TransAM ELISA

NF-κBp65, AP-1, and ATF2 DNA binding activity was analyzed by TransAM ELISA according to the manufacturer's protocol (Active Motif). Bound transcription factors were visualized by addition of a primary Ab directed against NF-κBp65, AP-1, or ATF2 elements, followed by detection with a HRP-conjugated secondary Ab. Absorbances were read at 450 nm with a reference wavelength of 655 nm. For the NF-κB and AP-1 assays, a protein standard curve was performed using recombinant NF-κBp65 or c-Jun recombinant protein to quantitate transcription factor levels in the protein samples.

Western blot

Cells were lysed in lysis buffer (Cell Signaling) supplemented with protease inhibitors (Roche), and protein concentrations were determined using the Bradford Protein Assay (Pierce, Rockford, IL) according to the manufacturer's protocol. Samples were stored at -20°C before use. Proteins (2.5 mg/ml per lane) were separated on 4–12% Bis-Tris gels (Invitrogen) and transferred onto Hybond-ECL nitrocellulose membranes (Amersham, Arlington Heights, IL) via a semidry blotting system (Thermo Fisher Scientific). The membranes were blocked and probed with primary Abs directed against STAT1 phosphorylated at tyrosine 701 (clone: D4A7), STAT1 phosphorylated at serine 727 (polyclonal), or total STAT1 (clone: 42H3; all Cell Signaling), followed by anti-rabbit-IgG-HRP AffiniPure Ab (Jackson ImmunoResearch Laboratories, Suffolk, U.K.) developed using Femto ECL substrate (Pierce) and quantitated with the ChemiDoc MP system (Bio-Rad).

Statistics

GraphPad Prism 4.0b (GraphPad Software, San Diego, CA) was used for statistical analysis. Principal component and redundancy analysis was

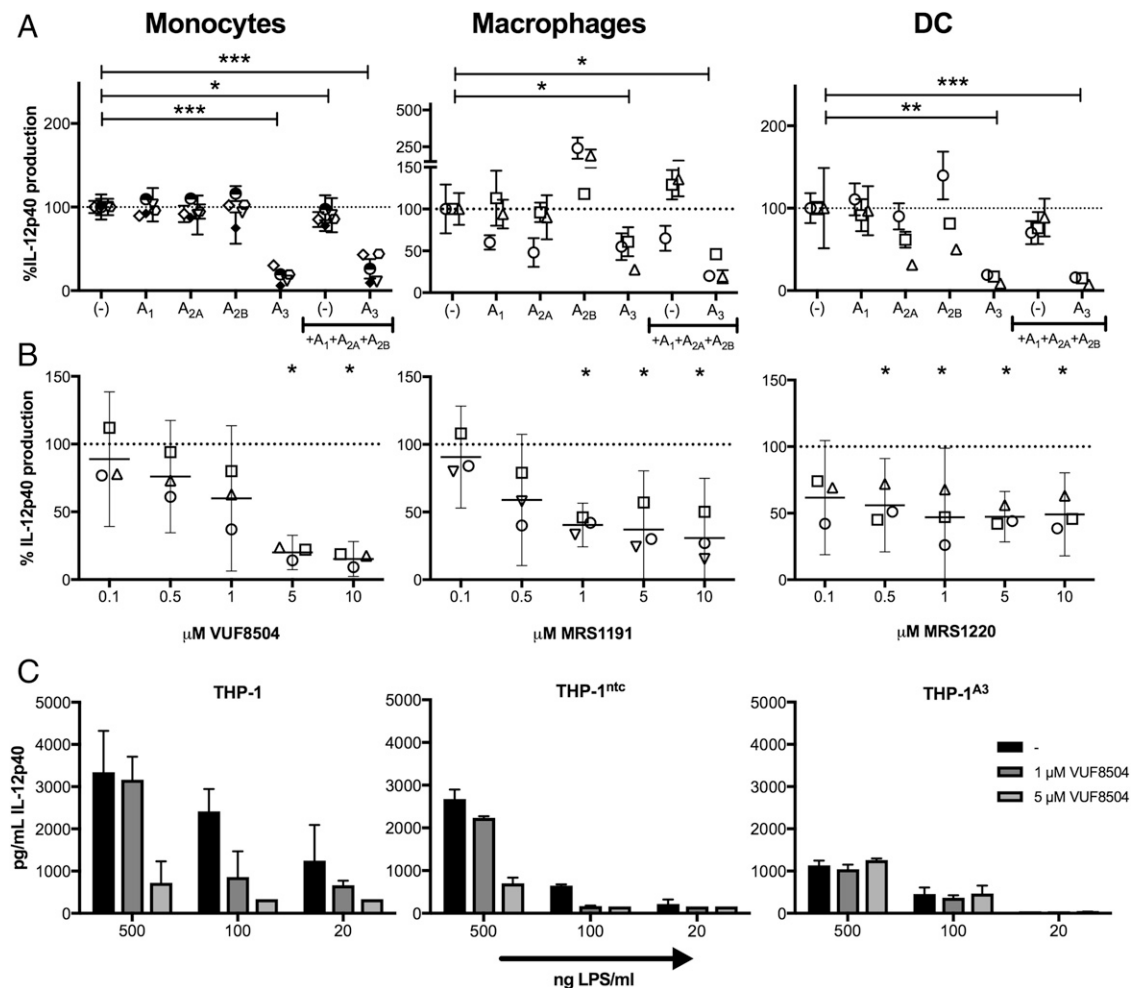


FIGURE 1. LPS-induced IL-12p40 is dependent on A₃R-mediated signaling. **(A)** Monocytes, monocyte-derived macrophages, and monocyte-derived DC were exposed for 16 h to 100 ng LPS/ml in the presence or absence of 1 μM A₁R, A_{2A}R, A_{2B}R, or A₃R antagonist either alone or in combination. IL-12p40 levels are expressed relative to production after exposure to LPS alone. Different symbols represent different donors. (dotted line = 100%, **p* < 0.05, ***p* < 0.01, ****p* < 0.001 paired *t* tests against LPS-exposed controls, SD are derived from measurements in triplicate). **(B)** Monocyte-derived DC from three donors were exposed for 16 h to 100 ng LPS/ml in the presence or absence of A₃R antagonists VUF8504, MRS1220, or MRS1191. Different symbols represent different donors. Horizontal lines indicate mean values with 95% confidence intervals. IL-12p40 levels are expressed relative to production after exposure to LPS alone (dotted line = 100%, **p* < 0.05 paired *t* tests against LPS-exposed controls). **(C)** IL-12p40 levels induced by exposure to different concentrations of LPS in THP-1 cells, in THP-1 cells transduced with nontargeting control (ntc) shRNA (THP-1^{ntc}), or in THP-1 cells transduced with A₃R-targeting shRNA (THP-1^{A3}) in the presence or absence of 1 or 5 μM VUF8504.

performed using Canoco 5.02 (Microcomputer Power, Ithaca, NY) at default settings.

Results

LPS-induced IL-12p40 production in monocytes, monocyte-derived macrophages, and DC is dependent on A₃R-mediated signaling

Recently, we published on the complex interplay between A_{2A}R and A₃R as modulators of innate immune responses (14). Our data

also suggested that A₃R-mediated signaling was directly involved in TLR-induced IL-12 production by myeloid cells. To investigate this, human monocytes, monocyte-derived macrophages, and monocyte-derived DC were exposed to the TLR4 agonist LPS in the absence or presence of specific ADORA antagonists. The presence of ADORA antagonists alone did not induce measurable levels of IL-12p40 in any of the cell types, whereas exposure to LPS induced the production of variable amounts of IL-12p40 in different cell types (Supplemental Table I). The presence of an

Table I. Primer and probe sequences

Target	Forward Primer (5'-3')	Reverse Primer (5'-3')	Probe
TNF-α	5'-CAGCCTCTTCTCCTTCTCTGAT-3'	5'-GCCAGAGGGCTGATTAGAGA-3'	GGCAGAAG
IL-12p40	5'-CCCTGACATTCTGCGTTCA-3'	5'-AGGTCTTGTCGGTGAAGACTCTA-3'	CCAGGGCA
IL-12p35	5'-CACTCCCAAAACCTGCTGAG-3'	5'-TCTCTTCAGAAGTGCAAGGTA-3'	TCTGGAGC
IL-12p19	5'-TGTTCCTCCATATCCAGTGTG-3'	5'-TCCTTTGCAAGCAGAAGCTGA-3'	CACAGCCA
MT1A	5'-GCAAAATGCAAGAGTGCAAAAT-3'	5'-GCACACTTGGCACAGCTC-3'	CTGCTCCT
MT1H	5'-TGGAAGTCCAGTCTCACCT-3'	5'-TGCATTGCACTTTTTCAC-3'	CTGCTCCT
MT2A	5'-AACCTGTCCGACTCTAGCC-3'	5'-GCAGGTGCAGGAGTCACC-3'	CTGCTCCT
MT3	5'-AAGTGCAGGGATGCAAAAT-3'	5'-CTGCACTTCTCTGCTTCTGC-3'	CTGCTCCT
GAPDH	5'-AGCCACATCGCTCAGACAC-3'	5'-GCCCAATACGACCAATCC-3'	CTTCCCA

Table II. IL-12p40 production values in picograms per milliliter per donor

+ 100 ng LPS/ml	μM	Donor 1		Donor 2		Donor 3	
		pg/ml	SD	pg/ml	SD	pg/ml	SD
VUF8504	0	79,436	22,939	106,007	26,507	54,163	5,941
	0.1	60,980	36,049	134,561	44,785	42,202	1,694
	0.5	48,134	29,284	119,011	17,470	39,546	344
	1	29,440	4,873	99,952	16,915	34,026	2,160
	5	11,316	4,198	85,177	23,751	12,865	2,480
	10	7,361	1,294	19,794	6,849	9,532	368
MRS1191	0	94,776	39,350	102,135	18,130	54,163	5,941
	0.1	79,206	11,822	110,306	19,756	43,261	589
	0.5	37,929	2,364	80,687	9,873	31,387	1,228
	1	40,010	4,726	46,819	3,052	18,038	246
	5	28,295	12,329	58,197	898	13,160	638
	10	25,627	7,262	51,231	5,206	8,282	2,676
MRS1220	0	79,436	22,939	106,007	26,507	43,119	2,485
	0.1	33,076	916	78,734	11,554	29,837	1,814
	0.5	40,191	7,182	47,498	13,639	30,981	2,005
	1	20,762	5,056	49,623	10,885	29,233	6,664
	5	35,090	1,733	44,056	4,484	24,199	2,540
	10	30,642	5,956	48,476	5,161	27,145	734

Detection level limit was 100 pg/ml.

A₃R antagonist significantly inhibited LPS-induced IL-12p40 production in monocytes, macrophages, and DC, whereas antagonizing A₁R, A_{2A}R, or A_{2B}R did not significantly affect the production of IL-12p40 in any of the cell types (Fig. 1A). An important role for A₃R-mediated signaling in LPS-induced IL-12p40 was confirmed by using combinations of different antagonists (Fig. 1A).

To validate that the observed effects were attributable to A₃R-mediated signaling, DC were stimulated with LPS in the presence of different concentrations of three structurally unrelated A₃R antagonists (Table II). All A₃R antagonists significantly inhibited LPS-induced IL-12p40 production (Fig. 1B). Finally, we silenced A₃R expression in THP-1 cells (THP-1 cells transduced with A₃R-targeting shRNA [THP-1^{A3}]) with lentiviral shRNA and measured LPS-induced IL-12p40 production. A₃R knockdown was >90% as confirmed by quantitative RT-PCR (Supplemental Fig. 1). LPS-induced IL-12p40 levels in THP-1^{A3} cells were decreased compared with those in THP-1 cells or in THP-1 cells transduced with nontargeting control (ntc) shRNA (THP-1^{ntc}; Fig. 1C). In contrast to THP-1 and THP-1^{ntc} cells, exposure of THP-1^{A3} cells to an A₃R antagonist had no effects on LPS-induced IL-12p40 production (Fig. 1C), confirming the specific involvement of A₃R-mediated signaling.

A₃R-mediated signaling is necessary to trigger the production of IL-12p40 and CCL2 in DC by multiple TLRs as well as by whole pathogens

We next characterized the involvement of A₃R-mediated signaling on IL-12p40 production as induced by other TLRs that are expressed by DC. Engagement of TLR2, 3, 4, 5, and 8 on DC from four donors induced the production of variable levels of IL-12p40 (Table III). Exposure of DC to TLR ligands in the presence of an A₃R antagonist significantly reduced TLR2, TLR3, TLR4, TLR5, and TLR8-induced IL-12p40 levels (Fig. 2A), demonstrating that A₃R-mediated signaling is broadly involved in TLR-induced IL-12p40 production. It should, however, be noted that although the qualitative aspect of the contribution of A₃R-mediated signaling to TLR responses is clear, effect sizes vary considerably between different TLR as well as between different donors.

To expand our analyses to other TLR-induced soluble factors, we choose to evaluate the effects of A₃R-mediated signaling on the robust cytokine responses induced by TLR4 and TLR8 ligands on DC from three different donors using Luminex technology. Exposure to TLR4 and TLR8 ligands triggered the production of multiple soluble factors (Fig. 2B). When the inhibition of A₃R-mediated signaling was analyzed against normalized TLR-induced cytokine production from different donors, only IL-12p40 and

Table III. IL-12p40 production values in picograms per milliliter per donor

Stimulus	Donor 1		Donor 2		Donor 3		Donor 4	
	pg/ml	SD	pg/ml	SD	pg/ml	SD	pg/ml	SD
+Pam ₃ CSK4	1,292	105	1,906	307	17,984	1,545	5,304	1,889
+Pam ₃ CSK4+VUF	364	108	1,496	972	6,073	1,223	125	68
+Poly(I:C)	2,918	311	1,574	525	4,082	372	1,140	378
+Poly(I:C)+VUF	983	234	890	165	2,402	224	759	276
+LPS	47,745	3,508	172,130	5,853	45,866	3,580	74,871	10,338
+LPS+VUF	6,417	493	84,546	22,682	26,547	2,318	7,359	481
+Flagellin	8,179	429	3,229	746	5,499	1,683	1,748	168
+Flagellin+VUF	1,647	1,050	930	213	3,461	1,044	110	9
+CL075	30,970	9,750	76,674	17,068	117,767	9,501	39,910	15,462
+CL075+VUF	16,862	4,383	21,397	8,437	64,751	14,621	4,444	1,910

Detection level limit was 100 pg/ml. DC were exposed to different TLR ligands in the absence or presence of the A₃R antagonist VUF8504.

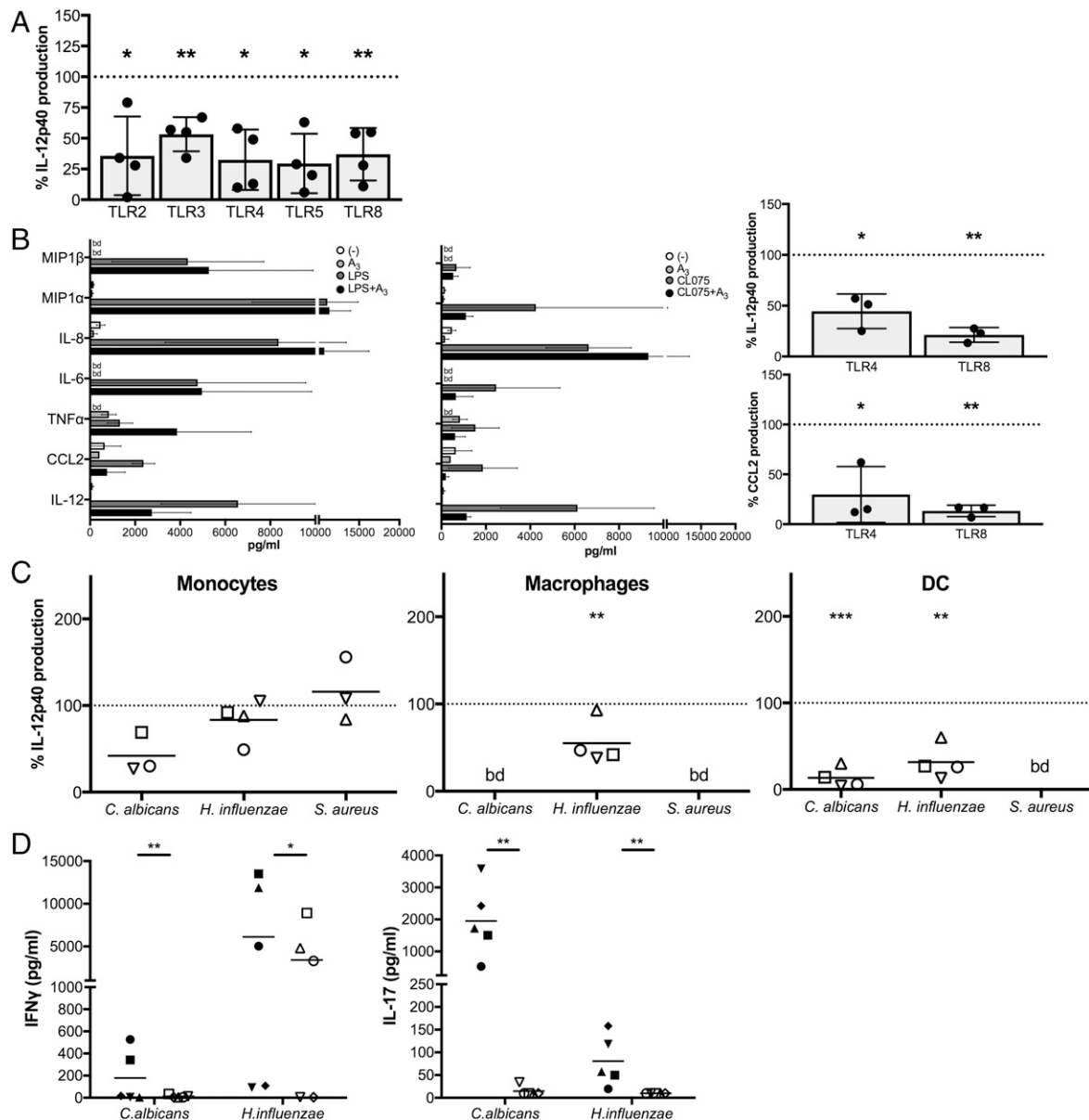


FIGURE 2. A₃R-mediated signaling is broadly involved in the TLR-induced production of IL-12p40 and CCL2. **(A)** Monocyte-derived DC of four different donors were exposed for 16 h to different TLR ligands in the absence or presence of 5 μ M VUF8504. For each TLR ligand, IL-12p40 levels in the presence of VUF8504 are expressed relative to production after exposure to each TLR ligand alone (dotted line = 100%, dots represent different donors, bars represent mean values (+ and - SD, calculated from four different means) of normalized response levels. TLR ligands used were 100 ng PAM₃CSK₄/ml (TLR2), 20 ng poly(I:C)/ml (TLR3), 100 ng LPS/ml (TLR4), 100 ng flagellin/ml (TLR5), or 1 μ g CL075/ml (TLR8). * p < 0.05, ** p < 0.01 paired t tests against TLR-exposed controls. **(B)** Luminex analysis of cell culture supernatants of DC from three donors exposed to 100 ng LPS/ml (TLR4, left panel) or 1 μ g CL075/ml (TLR8, middle panel) in the absence or presence of 5 μ M VUF8504. Bars represent mean values (+ and - SD, calculated from data from three different donors). In the right panels, IL-12p40 levels (upper panel) and CCL2 levels (lower panel) in the presence of VUF8504 are expressed relative to production after exposure to each TLR ligand alone (dotted line = 100%, dots represent different donors, bars indicate mean values of normalized response levels, SD were calculated from three different means, * p < 0.05, ** p < 0.01 paired t tests against TLR-exposed controls). **(C)** Monocytes, monocyte-derived macrophages, and monocyte-derived DC of four different donors were exposed for 16 h to whole pathogens (multiplicity of infection of 10) in the absence or presence of 5 μ M VUF8504. Different symbols represent different donors. IL-12p40 levels are expressed relative to production after exposure to corresponding pathogens alone (dotted line = 100%, * p < 0.05, ** p < 0.01 paired t tests against controls). **(D)** Monocyte-derived DC of five different donors (represented by different symbols) were exposed to different pathogens in the absence (closed symbols) or presence (open symbols) of 5 μ M VUF8504 and cocultured with donor-matched CD4⁺ T cells in a ratio of 5:1. IFN- γ levels were measured after 24 h, and IL-17 levels were measured after 5 d. Horizontal bars indicate the means (* p < 0.05, ** p < 0.01, *** p < 0.001, paired t tests on ¹⁰log-transformed data). bd, below detection levels.

CCL2 were significantly affected (Fig. 2B, right panels, Table IV). Exposure of DC to TLR2, -3, and -5 ligands in the presence of an A₃R antagonist also reduced CCL2 levels (data not shown), demonstrating that the effects were not limited to TLR4- and TLR8-induced responses.

Subsequently, we investigated the contribution of A₃R-mediated signaling to responses induced by whole pathogens that contain multiple ligands for innate immune receptors. We exposed monocytes, monocyte-derived macrophages, and monocyte-derived DC of four different donors to the fungus *C. albicans* as well as to

Table IV. Cytokine production values in picograms per milliliter per donor as determined by Luminesx

	Donor 1	Donor 2	Donor 3
IL12p40			
+LPS	9,211	2,707	7,791
+LPS +VUF8504	4,730	1,546	1,960
+CL075	4,708	10,065	3,605
+CL075+VUF8504	1,076	1,349	991
CCL2			
+LPS	1,798	2,699	2,619
+LPS +VUF8504	272	1,676	316
+CL075	293	1,900	3,396
+CL075+VUF8504	49	315	229

Detection level limit was 30 pg/ml.

Gram-negative *H. influenzae* and Gram-positive *S. aureus* bacteria in the absence or presence of an A₃R antagonist and measured IL-12p40 production. Monocytes produced relatively low levels (Supplemental Table II) of IL-12p40 in response to *C. albicans* and even lower levels when A₃R-mediated signaling was antagonized (Fig. 2C). Although exposure to *H. influenzae* potentially triggered the production of IL-12p40 in all four donors, and *S. aureus* triggered detectable production of IL-12p40 in three donors, these responses were not significantly affected when A₃R-mediated signaling was inhibited. Macrophages of all four donors produced detectable levels of IL-12p40 in response to *H. influenzae* only (Supplemental Table II), which were significantly lower when A₃R-mediated signaling was inhibited. In DC, *C. albicans* and *H. influenzae* potentially induced IL-12p40 production, whereas exposure to *S. aureus* did not induce detectable levels of IL-12p40 (Supplemental Table II). Both *C. albicans*- and *H. influenzae*-induced IL-12p40 responses were significantly inhibited when A₃R-signaling was antagonized (Fig. 2C).

The IL-12p40 subunit can heterodimerize with p35 or p19 to form bioactive IL-12 or IL-23 respectively. IL-12 is an important factor in the polarization of T cells to Th1 cells and the consequent production of IFN- γ , whereas IL-23 is involved in the polarization to Th17 cells and the consequent production of IL-17 (17). To examine whether blocking A₃R-mediated signaling could affect downstream T cell cytokine production, DC from five different donors were exposed to *C. albicans* and *H. influenzae* in the presence or absence of A₃R antagonist and coincubated with autologous CD4⁺ T cells for 5 d. Analysis of cell culture supernatants reveals that exposure to *H. influenzae* potentially induced IFN- γ , whereas exposure to *C. albicans* mainly induced the production of IL-17 (Fig. 2D). There was considerable donor-donor variation, and it is interesting to note that the two donors that were poor IFN- γ producers were the ones that produced the highest levels of IL-17. When A₃R signaling was antagonized, both IFN- γ and IL-17 responses were significantly lower with larger effect sizes on IL-17 responses (Fig. 2D). Future experiments will further focus on the implications of these differences.

A₃R-mediated signaling enhances LPS-induced phosphorylation of STAT1 at tyrosine 701

A₃R-mediated signaling affected IL-12 and CCL2 production at the transcription level, as LPS-induced IL-12p40- and CCL2-encoding mRNA levels in DC in the presence of an A₃R antagonist were 5- and 39-fold lower, respectively (Fig. 3A, Table I). In addition, LPS-induced mRNA levels of IL-12p35 and IL-23p19 subunits were both ~5-fold lower when A₃R-mediated signaling was antagonized. Interestingly, exposure of cells to A₃R antagonist alone already decreased basal mRNA expression levels of the IL-12p40 (to a mean of 23%) and p35 (to a mean of 65%) subunits

as well as of CCL2 (to a mean of 14%), suggesting a role for homeostatic A₃R-mediated signaling in DC. To delineate how A₃R-mediated signaling affects TLR-induced intracellular signaling cascades, we first assessed LPS-induced phosphorylation levels of the NF- κ B at serine 536 by PathScan ELISA, an important TLR-induced modulator of transcriptional activity (18). This was not affected by antagonizing A₃R-mediated signaling, and in accordance, NF- κ B binding to its consensus site as assessed by TransAM ELISA was similar in nuclear extracts of DC exposed to LPS both in the absence or presence of an A₃R antagonist (Fig. 3B, 3C). In addition to activation of NF- κ B (19), TLR-induced signaling activates several MAPKs. We therefore used PathScan ELISA to evaluate phosphorylation levels of SAPK/JNK, ERK1/2, and p38 in cellular lysates of DC exposed to LPS in the absence or presence of an A₃R antagonist. Whereas LPS-induced levels of p-ERK1/2 and p-p38 were unaffected, LPS-induced p-SAPK/JNK levels were decreased at early time points in the presence of an A₃R antagonist (Fig. 3D). SAPK/JNK induces activation of the transcription factor AP-1. However, LPS-induced c-Jun, c-Fos, and ATF2 binding levels were not significantly different in nuclear extracts of DC exposed to LPS in the presence of an A₃R antagonist (Fig. 3E), rendering it unlikely that differences in SAPK/JNK phosphorylation underlie the observed effects on IL-12 and CCL2 production.

Next to binding sites for NF- κ B and AP-1 elements, the promoter regions of IL-12p40 and CCL2 also share binding sites for STAT1. Full activation of STAT1 requires phosphorylation at serine 727 and tyrosine 701. Whereas LPS-induced phosphorylation of STAT1 at S727 was unaffected in the presence of an A₃R antagonist, LPS-induced phosphorylation of STAT1 at Y701 was strongly decreased after 60 min of stimulation (Fig. 3F). To confirm the involvement of STAT1 tyrosine 701 phosphorylation, we tested whether the reduced levels of LPS-induced IL-12p40 in the presence of an A₃R antagonist could be rescued by the addition of IFN- γ , a well-known inducer of STAT1 tyrosine 701 phosphorylation (20). Confirming our earlier results, IFN- γ partially restored LPS-induced IL-12p40 levels in the presence of an A₃R antagonist (Fig. 3G).

A₃R-mediated signaling inhibits metallothionein expression levels

Finally, we submitted mRNA samples of DC exposed to LPS in the presence or absence of an A₃R antagonist to total transcriptome analysis by RNA sequencing (<https://www.ncbi.nlm.nih.gov/geo/query/acc.cgi?acc=GSE125747>). Principal component analysis of the samples (Fig. 4A) demonstrates a clear separation of the different sample classes according to stimulation conditions, which was confirmed by redundancy analysis ($p < 0.002$; data not shown). Venn diagrams illustrate the overlap between different sample groups (Fig. 4B). Differential gene expression analysis demonstrates that exposure to LPS significantly (adjusted $p < 0.01$) altered the expression levels of 4,893 gene transcripts (GSE125747), whereas exposure to an A₃R antagonist altered the expression levels of 381 gene transcripts only (Table V). Expression levels of 146 transcripts were significantly different between cells exposed to LPS alone or in combination with an A₃R antagonist (GSE125747). Analysis of the individual transcripts reveals that exposure to an A₃R antagonist, even in the absence of LPS activation, leads to a strong increase of metallothionein mRNA levels (the top 13 genes with the lowest p values are all metallothionein genes). These findings were confirmed for four metallothionein isoforms by quantitative RT-PCR (Fig. 4C, Table I). In addition, the data confirm that LPS-induced CCL2 and IL-12 (NS) mRNA levels were lower in the presence of an A₃R antagonist (GSE125747).

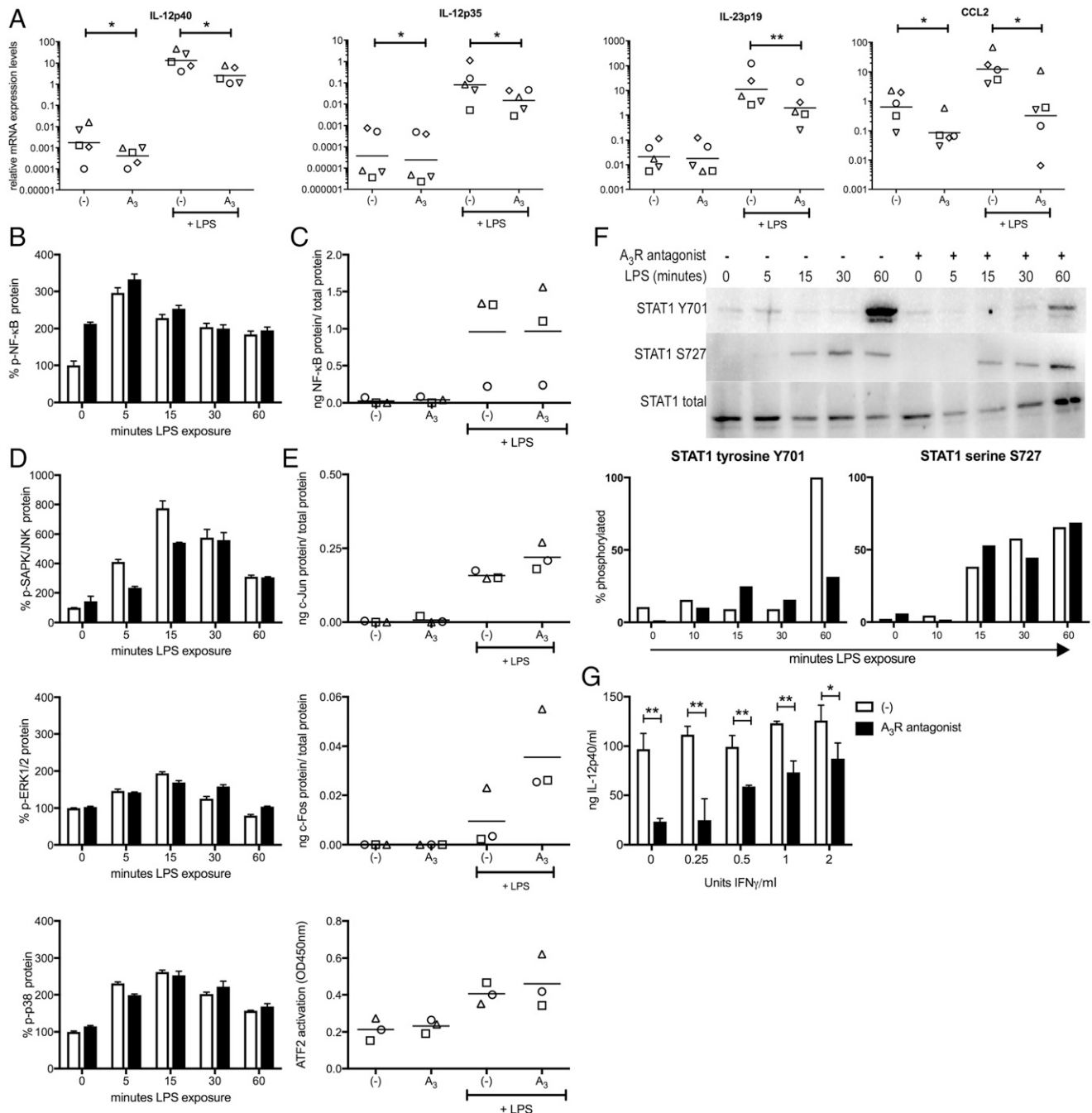


FIGURE 3. A₃R-mediated signaling is necessary to induce phosphorylation of STAT1 tyrosine 701. **(A)** Monocyte-derived DC were exposed for 6 h to 500 ng LPS/ml in the presence or absence of 5 μ M VUF8504, and mRNA levels encoding for IL-12p40, CCL2, IL-12p35, and IL-23p19 were quantified by real-time RT-PCR and standardized to GAPDH mRNA expression levels. Different symbols represent different donors. In the graph, relative expression levels are given on a 10^{\log} scale ($*p < 0.05$, $**p < 0.01$ paired t tests on the 10^{\log} -transformed data). **(B)** Phosphorylated NF- κ B protein levels in cellular lysates of monocyte-derived DC exposed to 500 ng LPS/ml for 0, 5, 15, 30, or 60 min in the presence or absence of 5 μ M VUF8504. Samples were standardized to total NF- κ B levels. A representative example of three different donors is shown. **(C)** Bound NF- κ B levels in nuclear lysates of monocyte-derived DC exposed to 500 ng LPS/ml for 1 h in the presence or absence of 5 μ M VUF8504. Different symbols represent different donors. **(D)** Phosphorylated ERK1/2, p38, SAPK/JNK protein levels in cellular lysates of monocyte-derived DC exposed to 500 ng LPS/ml for 0, 5, 15, 30, or 60 min in the presence or absence of 5 μ M VUF8504. Samples were standardized to NF- κ B levels. A representative example of three different donors is shown. **(E)** Different symbols represent different donors. Bound c-Jun, c-Fos, and ATF2 levels in nuclear lysates of monocyte-derived DC exposed to 500 ng LPS/ml for 1 h in the presence or absence of 5 μ M VUF8504 ($*p < 0.05$ paired t tests for A₃R-mediated effects). **(F)** Western blot analysis of phosphorylated STAT1 serine 727 and tyrosine 701 in monocyte-derived DC exposed to 500 ng LPS/ml for 0, 5, 15, 30, or 60 min in the presence or absence of 5 μ M VUF8504. Samples were standardized to total STAT1 levels and quantitated (lower panels). A representative example of three different donors is shown. **(G)** A representative example of three different donors is shown. Monocyte-derived DC were exposed to 500 ng LPS/ml for 16 h in the presence or absence of 5 μ M VUF8504 and of increasing concentrations of IFN- γ ($*p < 0.05$, $**p < 0.01$ paired t tests for A₃R-mediated effects).

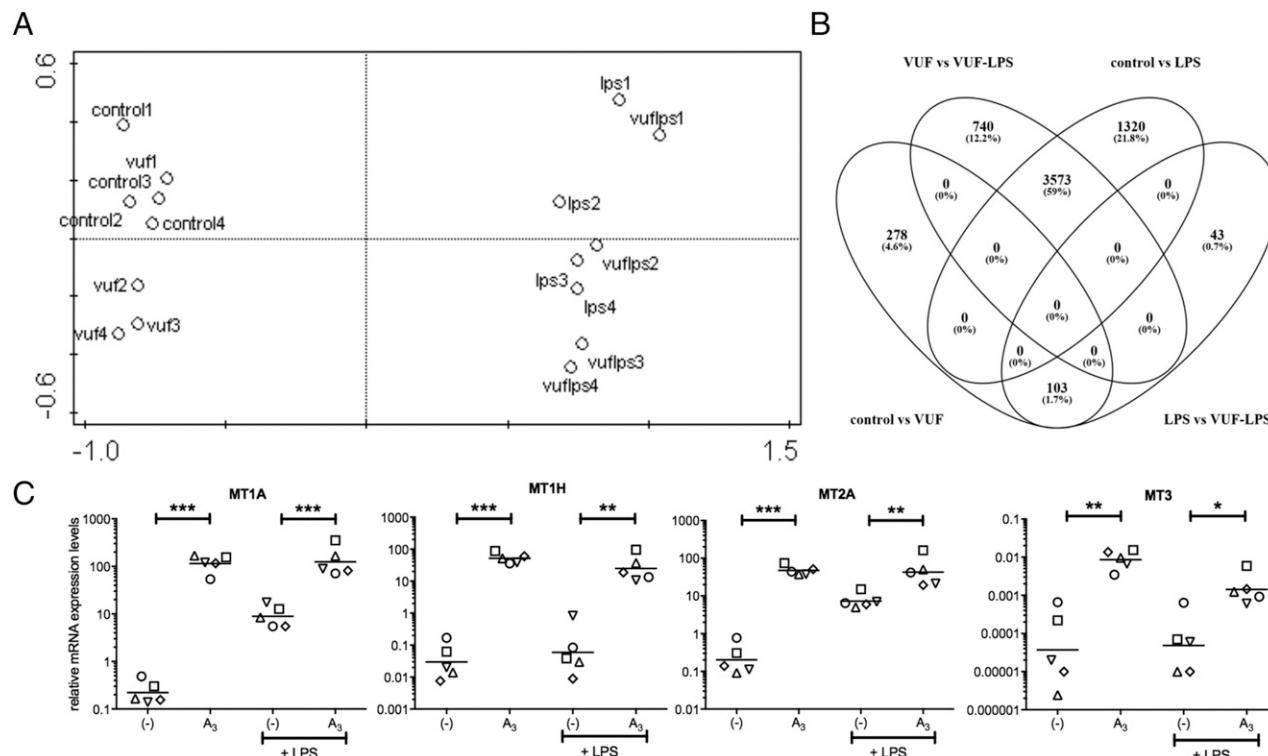


FIGURE 4. Analysis of the mRNA transcriptome reveals the involvement of metallothioneins in A₃R-mediated signaling. **(A)** Principal component analysis of mRNA transcriptomes from monocyte-derived DC from four human donors exposed for 6 h to 500 ng LPS/ml in the presence or absence of 5 μ M VUF8504. The x-axis explains 65% of the variation, and the y-axis explains 7% of the variation. **(B)** Venn diagrams demonstrating overlaps in differentially expressed genes between the sample groups. **(C)** Monocyte-derived DC were exposed for 6 h to 500 ng LPS/ml in the presence or absence of 5 μ M VUF8504, and MT1A-, MT1H-, MT2A-, and MT3-encoding mRNA expression levels were quantified by real-time RT-PCR and standardized to GAPDH mRNA expression levels. Different symbols represent different donors. In the graph, relative expression levels are given on a ¹⁰log scale (**p* < 0.05, ***p* < 0.01, ****p* < 0.001 paired *t* tests on the ¹⁰log-transformed data).

Discussion

In this study, we demonstrate that A₃R-mediated signaling is critically involved in LPS-induced IL-12 production by myeloid cells. Further analysis of DC demonstrates that also CCL2 production as induced by a broad range of TLR ligands or whole pathogens was affected. A₃R-mediated signaling suppresses metallothionein expression levels and amplifies TLR-induced phosphorylation of the transcription factor STAT1 at tyrosine 701, demonstrating a complex and novel layer of regulation of innate immune responses. To our knowledge, we are the first to describe a role for endogenously produced extracellular adenosine and A₃R-mediated signaling in the initiation of TLR-induced cytokine responses.

Extracellular adenosine can interact with four different ADORA subtypes. Interestingly, A₃R expression levels are rapidly down-regulated after TLR-mediated activation of myeloid cells, whereas expression levels of A_{2A}R are strongly enhanced (14). Previously, we have hypothesized that this shift in ADORA expression pattern underlies the inhibitory effects of extracellular adenosine on TLR-mediated cytokine production by unleashing the full capacity of A_{2A}R-mediated anti-inflammatory signaling. This study suggests that downregulation of A₃R also has direct anti-inflammatory effects by depriving TLR-activated myeloid cells of their capacity to produce IL-12 and CCL2. We did not find evidence for direct effects on Ag presentation capacity, as the LPS-induced increase of cell surface expression levels of receptors involved in Ag presentation by DC was unaffected by exposure to an A₃R antagonist (Supplemental Fig. 2).

Our transcriptome data revealed that A₃R-mediated effects not only modulated TLR-induced signaling but also affected

otherwise unstimulated cells. Most striking was the strong induction of metallothioneins when homeostatic A₃R-mediated signaling was inhibited. Metallothioneins are low m.w. cysteine-rich proteins that regulate intracellular zinc homeostasis, detoxify heavy metals, and counteract superoxide stress (21). Their expression is potently induced by metal exposure and oxidative stress but also by cytokine signaling and microbial challenge (22–25). In myeloid cells, there is ample evidence for an important role of metallothioneins in the maintenance of intracellular zinc homeostasis (26–28). Manipulation of intracellular and extracellular zinc levels can be used to modulate the phenotype of myeloid cells (29–31), and different studies have identified a role for zinc signaling in kinase and phosphatase functions (32, 33). Interestingly, a recent study demonstrated that metallothioneins inhibit the phosphorylation of STAT1 and STAT3 (34). It has been postulated that metallothionein 1 and 2 sequester intracellular zinc, thereby sustaining protein tyrosine phosphatase 1B activity that in turn dephosphorylates STATs (32, 33).

The promoter regions of IL-12p40 and CCL2 share binding sites for STAT1, and we have identified that TLR-induced phosphorylation of STAT1 at tyrosine 701 was strongly reduced when A₃R-mediated signaling was inhibited. More pathways may be involved, as IFN- γ -induced phosphorylation of STAT1 tyrosine 701 only partially restored TLR-induced IL-12p40 levels in the presence of an A₃R antagonist (Fig. 3G). Although the complete elucidation of intracellular signaling cascades remains to be established, the involvement of the STAT1 pathway is evident. Together, this leads us to propose a novel molecular mechanism

Table V. Selection of significantly differentially expressed transcripts

Gene ID	Control	VUF8504	VUF8504/Control	<i>p</i> Value	Protein
Upregulated					
ENSG00000205358	7.12	21,350.49	2,997.39	4.17×10^{-281}	MT1H
ENSG00000125144	25.88	68,870.43	2,660.90	1.16×10^{-248}	MT1G
ENSG00000187193	29.30	22,074.37	753.32	6.58×10^{-244}	MT1X
ENSG00000233929	5.88	6,135.09	1,042.68	9.62×10^{-219}	MT1XP1
ENSG00000125148	104.41	54,901.37	525.81	4.82×10^{-205}	MT2A
ENSG00000260549	0	2,535.10	INF	1.62×10^{-125}	MT1L
ENSG00000244020	0.52	988.00	1,906.61	5.21×10^{-115}	MT1HL1
ENSG00000162840	10.28	7,672.82	746.13	2.20×10^{-100}	MT2P1
ENSG00000205364	0.73	26,587.48	36,440.65	7.38×10^{-76}	MT1M
ENSG00000169715	9.76	20,576.90	2,108.37	4.20×10^{-66}	MT1E
ENSG00000229230	0.26	3,222.95	12,272.09	3.21×10^{-56}	MT1P3
ENSG00000198417	12.49	8,660.24	693.20	5.69×10^{-45}	MT1F
ENSG00000205362	0	9,797.37	INF	5.01×10^{-33}	MT1A
ENSG00000197358	70.77	758.76	10.72	5.72×10^{-33}	BNIP3P1
ENSG00000177181	1.76	181.56	103.39	9.76×10^{-33}	RIMKLA
ENSG00000176171	105.96	957.69	9.04	3.81×10^{-32}	BNIP3
ENSG00000196739	4.62	197.23	42.70	5.50×10^{-32}	COL27A1
ENSG00000109762	107.88	1,322.26	12.26	1.48×10^{-30}	SNX25
ENSG00000108352	22.38	1,087.54	48.61	6.25×10^{-27}	RAPGEFL1
ENSG00000135766	1,143.40	5,965.38	5.22	3.31×10^{-25}	EGLN1
Downregulated					
ENSG00000196950	838.97	243.35	0.29	5.54×10^{-11}	SLC39A10
ENSG00000141655	5,982.98	2,691.38	0.45	5.71×10^{-7}	TNFRSF11A
ENSG00000171659	170.90	35.11	0.21	7.05×10^{-7}	GPR34
ENSG00000168906	7,886.25	3,700.90	0.47	4.88×10^{-6}	MAT2A
ENSG00000163563	1,851.51	784.99	0.42	6.66×10^{-6}	MNDA
ENSG00000100644	4,385.27	2,124.05	0.48	1.31×10^{-5}	HIF1A
ENSG00000164163	1,143.55	524.27	0.46	4.56×10^{-5}	ABCE1
ENSG00000095585	958.15	343.88	0.36	5.24×10^{-5}	BLNK
ENSG00000134242	717.17	306.51	0.43	6.58×10^{-5}	PTPN22
ENSG00000179041	1,604.57	773.89	0.48	1.79×10^{-4}	RRS1
ENSG00000145569	1,454.94	663.16	0.46	2.24×10^{-4}	FAM105A
ENSG00000187037	457.64	193.28	0.42	3.52×10^{-4}	GPR141
ENSG00000197442	2,218.70	1,171.86	0.53	4.37×10^{-4}	MAP3K5
ENSG00000164125	2,894.64	1,551.32	0.54	7.06×10^{-4}	FAM198B
ENSG00000168918	4,673.92	2,535.44	0.54	8.17×10^{-4}	INPP5D
ENSG00000075303	1,303.48	666.43	0.51	8.34×10^{-4}	SLC25A40
ENSG00000104549	1,598.28	825.70	0.52	8.87×10^{-4}	SQLE
ENSG00000164933	480.59	219.03	0.46	9.25×10^{-4}	SLC25A32
ENSG00000178105	260.35	106.77	0.41	1.02×10^{-3}	DDX10
ENSG00000196814	499.07	231.36	0.46	1.08×10^{-3}	MVB12B

Depicted are the top 20 of upregulated (top) and downregulated (bottom) transcripts (based on adjusted *p* values) after exposure to VUF8504. ID, identification; INF, infinite ratio as a result of expression levels below threshold in the reference samples.

that links adenosine-induced signaling via the metallothionein–zinc axis to modulation of innate and adaptive immune responses.

Extracellular adenosine is best known as an anti-inflammatory modulator, and A₃R-mediated signaling has previously been associated with the inhibition rather than with the initiation of LPS-induced IL-12 and/or TNF-α in different murine models and cell lines, as well as in human monocytes and U937 cells (35–40). Several factors may explain the discrepancies with our findings. First, the described inhibitory effects of A₃R-mediated signaling have primarily been observed in murine models and/or cells. Whereas the sequences of A₁R, A_{2A}R, and A_{2B}R are well conserved across species, A₃R sequences differ considerably. Sequence comparisons between rodent and human show 70–75% gene sequence homology and 85–87% protein sequence homology (6, 14). Second, there is evidence that G protein coupling of A₃R is different between rodents and humans. In A₃R-humanized mice, bone marrow–derived mast cells were unable to initiate conventional murine A₃R-mediated signaling pathways. This was attributed to sequence differences in the intracellular region of human A₃R, resulting in the uncoupling of murine G proteins (41). Third, discrepancies with observations in U937 cells might be attributable to the differentiation/transformed status of these cells.

In conclusion, we describe a new mechanism that is important for TLR-induced IL-12 and CCL2 responses. Because all experiments were performed in the absence of exogenous adenosine or other ADORA agonists, the observed effects were attributable to endogenously produced extracellular adenosine contributing to TLR-induced responses in an autocrine or paracrine manner. Interestingly, this mechanism bears resemblance to the mechanism regulating the production of inflammasome-induced IL-1β in which endogenous ATP acts as a similar signal through P2X7 receptors (42). Our data suggest that antagonizing A₃R signaling could selectively affect TLR-induced production of IL-12 and CCL2, thereby representing a novel immune modulatory strategy. However, given the widespread distribution of A₃R throughout the body (43), specific delivery to the site of inflammation represents an important challenge when considering such an approach.

Acknowledgments

We thank E. Remarque for expert assistance with the statistical analyses, S.B. Geutskens, M.E. Hoonakker, and B. 't Hart for critically reading the manuscript.

Disclosures

The authors have no financial conflicts of interest.

References

- Janeway, C. A., Jr., and R. Medzhitov. 2002. Innate immune recognition. *Annu. Rev. Immunol.* 20: 197–216.
- Akira, S., and K. Takeda. 2004. Toll-like receptor signalling. *Nat. Rev. Immunol.* 4: 499–511.
- Takeda, K., T. Kaisho, and S. Akira. 2003. Toll-like receptors. *Annu. Rev. Immunol.* 21: 335–376.
- Kawai, T., and S. Akira. 2005. Toll-like receptor downstream signaling. *Arthritis Res. Ther.* 7: 12–19.
- Iwasaki, A., and R. Medzhitov. 2004. Toll-like receptor control of the adaptive immune responses. *Nat. Immunol.* 5: 987–995.
- Fredholm, B. B., A. P. IJzerman, K. A. Jacobson, K. N. Klotz, and J. Linden. 2001. International Union of Pharmacology. XXV. Nomenclature and classification of adenosine receptors. *Pharmacol. Rev.* 53: 527–552.
- Jacobson, K. A., and Z. G. Gao. 2006. Adenosine receptors as therapeutic targets. *Nat. Rev. Drug Discov.* 5: 247–264.
- Fossetta, J., J. Jackson, G. Deno, X. Fan, X. K. Du, L. Bober, A. Soudé-Bermejo, O. de Bouteiller, C. Caux, C. Lunn, et al. 2003. Pharmacological analysis of calcium responses mediated by the human A₃ adenosine receptor in monocyte-derived dendritic cells and recombinant cells. *Mol. Pharmacol.* 63: 342–350.
- Panther, E., M. Idzko, Y. Herouy, H. Rheinen, P. J. Gebicke-Haerter, U. Mrowietz, S. Dichmann, and J. Norgauer. 2001. Expression and function of adenosine receptors in human dendritic cells. *FASEB J.* 15: 1963–1970.
- Haskó, G., D. G. Kuhel, J. F. Chen, M. A. Schwarzschild, E. A. Deitch, J. G. Mabley, A. Marton, and C. Szabó. 2000. Adenosine inhibits IL-12 and TNF- α production via adenosine A_{2A} receptor-dependent and independent mechanisms. *FASEB J.* 14: 2065–2074.
- Link, A. A., T. Kino, J. A. Worth, J. L. McGuire, M. L. Crane, G. P. Chrousos, R. L. Wilder, and I. J. Elenkov. 2000. Ligand-activation of the adenosine A_{2A} receptors inhibits IL-12 production by human monocytes. *J. Immunol.* 164: 436–442.
- Sands, W. A., A. F. Martin, E. W. Strong, and T. M. Palmer. 2004. Specific inhibition of nuclear factor-kappaB-dependent inflammatory responses by cell type-specific mechanisms upon A_{2A} adenosine receptor gene transfer. *Mol. Pharmacol.* 66: 1147–1159.
- Palmer, T. M., and M. A. Trevelthick. 2008. Suppression of inflammatory and immune responses by the A_{2A} adenosine receptor: an introduction. *Br. J. Pharmacol.* 153(Suppl. 1): S27–S34.
- van der Putten, C., E. A. Zuiderwijk-Sick, L. van Straalen, E. D. de Geus, L. A. Boven, I. Kondova, A. P. IJzerman, and J. J. Bajramovic. 2009. Differential expression of adenosine A₃ receptors controls adenosine A_{2A} receptor-mediated inhibition of TLR responses in microglia. *J. Immunol.* 182: 7603–7612.
- Harrison, A., D. W. Dyer, A. Gillaspay, W. C. Ray, R. Mungur, M. B. Carson, H. Zhong, J. Gipson, M. Gipson, L. S. Johnson, et al. 2005. Genomic sequence of an otitis media isolate of nontypeable *Haemophilus influenzae*: comparative study with *H. influenzae* serotype d, strain KW20. *J. Bacteriol.* 187: 4627–4636.
- Pfaffl, M. W. 2001. A new mathematical model for relative quantification in real-time RT-PCR. *Nucleic Acids Res.* 29: e45.
- Schmitt, N., and H. Ueno. 2015. Regulation of human helper T cell subset differentiation by cytokines. *Curr. Opin. Immunol.* 34: 130–136.
- Chen, L. F., and W. C. Greene. 2004. Shaping the nuclear action of NF-kappaB. *Nat. Rev. Mol. Cell Biol.* 5: 392–401.
- Vidya, M. K., V. G. Kumar, V. Sejian, M. Bagath, G. Krishnan, and R. Bhatta. 2018. Toll-like receptors: significance, ligands, signaling pathways, and functions in mammals. *Int. Rev. Immunol.* 37: 20–36.
- Schroder, K., P. J. Hertzog, T. Ravasi, and D. A. Hume. 2004. Interferon-gamma: an overview of signals, mechanisms and functions. *J. Leukoc. Biol.* 75: 163–189.
- Kimura, T., and T. Kambe. 2016. The functions of metallothionein and ZIP and ZnT transporters: an overview and perspective. *Int. J. Mol. Sci.* 17: 336.
- Hirano, T., M. Murakami, T. Fukada, K. Nishida, S. Yamasaki, and T. Suzuki. 2008. Roles of zinc and zinc signaling in immunity: zinc as an intracellular signaling molecule. *Adv. Immunol.* 97: 149–176.
- Mocchegiani, E., R. Giacconi, C. Cipriano, L. Costarelli, E. Muti, S. Tesei, C. Giuli, R. Papa, F. Marcellini, E. Mariani, et al. 2007. Zinc, metallothioneins, and longevity—effect of zinc supplementation: zincage study. *Ann. N. Y. Acad. Sci.* 1119: 129–146.
- Subramanian Vignesh, K., J. A. Landero Figueroa, A. Porollo, J. A. Caruso, and G. S. Deepe, Jr. 2013. Granulocyte macrophage-colony stimulating factor induced Zn sequestration enhances macrophage superoxide and limits intracellular pathogen survival. *Immunity* 39: 697–710.
- Subramanian Vignesh, K., J. A. Landero Figueroa, A. Porollo, S. Divanovic, J. A. Caruso, and G. S. Deepe, Jr. 2016. IL-4 induces metallothionein 3- and SLC30A4-dependent increase in intracellular Zn(2+) that promotes pathogen persistence in macrophages. *Cell Rep.* 16: 3232–3246.
- Subramanian Vignesh, K., J. A. Landero Figueroa, A. Porollo, J. A. Caruso, and G. S. Deepe, Jr. 2013. Zinc sequestration: arming phagocyte defense against fungal attack. *PLoS Pathog.* 9: e1003815.
- Kanekiyo, M., N. Itoh, A. Kawasaki, A. Matsuyama, K. Matsuda, T. Nakanishi, and K. Tanaka. 2002. Metallothionein modulates lipopolysaccharide-stimulated tumour necrosis factor expression in mouse peritoneal macrophages. *Biochem. J.* 361: 363–369.
- Subramanian Vignesh, K., and G. S. Deepe, Jr. 2017. Metallothioneins: emerging modulators in immunity and infection. *Int. J. Mol. Sci.* 18: 2197.
- Kanekiyo, M., N. Itoh, A. Kawasaki, K. Matsuda, T. Nakanishi, and K. Tanaka. 2002. Metallothionein is required for zinc-induced expression of the macrophage colony stimulating factor gene. *J. Cell. Biochem.* 86: 145–153.
- George, M. M., K. Subramanian Vignesh, J. A. Landero Figueroa, J. A. Caruso, and G. S. Deepe, Jr. 2016. Zinc induces dendritic cell tolerogenic phenotype and skews regulatory T cell-Th17 balance. *J. Immunol.* 197: 1864–1876.
- Kitamura, H., H. Morikawa, H. Kamon, M. Iguchi, S. Hojyo, T. Fukada, S. Yamashita, T. Kaisho, S. Akira, M. Murakami, and T. Hirano. 2006. Toll-like receptor-mediated regulation of zinc homeostasis influences dendritic cell function. *Nat. Immunol.* 7: 971–977.
- Haase, H., and L. Rink. 2014. Zinc signals and immune function. *Biofactors* 40: 27–40.
- Haase, H., and L. Rink. 2009. Functional significance of zinc-related signaling pathways in immune cells. *Annu. Rev. Nutr.* 29: 133–152.
- Wu, C., C. Pot, L. Apetoh, T. Thalhimer, B. Zhu, G. Murugaiyan, S. Xiao, Y. Lee, M. Rangachari, N. Yosef, and V. K. Kuchroo. 2013. Metallothioneins negatively regulate IL-27-induced type 1 regulatory T-cell differentiation. *Proc. Natl. Acad. Sci. USA* 110: 7802–7807.
- Sajjadi, F. G., K. Takabayashi, A. C. Foster, R. C. Domingo, and G. S. Firestein. 1996. Inhibition of TNF- α expression by adenosine: role of A₃ adenosine receptors. *J. Immunol.* 156: 3435–3442.
- Haskó, G., C. Szabó, Z. H. Németh, V. Kvetan, S. M. Pastores, and E. S. Vizi. 1996. Adenosine receptor agonists differentially regulate IL-10, TNF- α , and nitric oxide production in RAW 264.7 macrophages and in endotoxemic mice. *J. Immunol.* 157: 4634–4640.
- Martin, L., S. C. Pingle, D. M. Hallam, L. P. Rybak, and V. Ramkumar. 2006. Activation of the adenosine A₃ receptor in RAW 264.7 cells inhibits lipopolysaccharide-stimulated tumor necrosis factor- α release by reducing calcium-dependent activation of nuclear factor-kappaB and extracellular signal-regulated kinase 1/2. *J. Pharmacol. Exp. Ther.* 316: 71–78.
- McWhinney, C. D., M. W. Dudley, T. L. Bowlin, N. P. Peet, L. Schook, M. Bradshaw, M. De, D. R. Borchering, and C. K. Edwards, III. 1996. Activation of adenosine A₃ receptors on macrophages inhibits tumor necrosis factor- α . *Eur. J. Pharmacol.* 310: 209–216.
- Szabó, C., G. S. Scott, L. Virág, G. Egnaczky, A. L. Salzman, T. P. Shanley, and G. Haskó. 1998. Suppression of macrophage inflammatory protein (MIP)-1 α production and collagen-induced arthritis by adenosine receptor agonists. *Br. J. Pharmacol.* 125: 379–387.
- la Sala, A., M. Gadina, and B. L. Kelsall. 2005. G(i)-protein-dependent inhibition of IL-12 production is mediated by activation of the phosphatidylinositol 3-kinase-protein 3 kinase B/Akt pathway and JNK. *J. Immunol.* 175: 2994–2999.
- Yamano, K., M. Inoue, S. Masaki, M. Saki, M. Ichimura, and M. Satoh. 2006. Generation of adenosine A₃ receptor functionally humanized mice for the evaluation of the human antagonists. *Biochem. Pharmacol.* 71: 294–306.
- Kahlenberg, J. M., K. C. Lundberg, S. B. Kertesz, Y. Qu, and G. R. Dubyak. 2005. Potentiation of caspase-1 activation by the P2X₇ receptor is dependent on TLR signals and requires NF-kappaB-driven protein synthesis. *J. Immunol.* 175: 7611–7622.
- Salvatore, C. A., M. A. Jacobson, H. E. Taylor, J. Linden, and R. G. Johnson. 1993. Molecular cloning and characterization of the human A₃ adenosine receptor. *Proc. Natl. Acad. Sci. USA* 90: 10365–10369.